DOI: 10.1002/chem.200900688

Is the Backbone Conformation of C^{α}-Methyl Proline Restricted to a Single Region?

Matteo De Poli,[a] Alessandro Moretto,[a] Marco Crisma,[a] Cristina Peggion,[a] Fernando Formaggio,[a] Bernard Kaptein,[b] Quirinus B. Broxterman,[b] and Claudio Toniolo*[a]

Dedicated to the Centenary of the Italian Chemical Society

Abstract: C^{α}-Methyl-L-proline, or L-(αMe)Pro, is probably the most conformationally constrained α-amino acid. In particular, its ω and ϕ torsion angles are restricted to about 180 and −60°, respectively, and only three ranges of values are theoretically available for ψ in mono- or longer peptides, namely, about −30° (*cis*′, 3_{10}/α-helical structure), 60° (inverse γ turn), or 140° (*trans*′, poly(L-Pro)$_n$ II structure). In this work, we examined the tendency of a number of N^{α}-acyl dipeptide N′-alkylamides of the type RCO-(αMe)Pro-Xxx-NHR′ or RCO-Xxx-(αMe)Pro-NHR′, in which Xxx is L (or D)-Ala, Aib (α-aminoisoburyric acid), or L (or D)-(αMe)Pro, long enough to fold into intramolecularly hydrogen-bonded γ or β turns. The results are compared with those obtained for the corresponding dipeptides based on Pro, a well-known turn-forming residue. For the crystal-state 3D-structural analysis we used X-ray diffraction, whereas our solution conformational analysis was heavily based on the FTIR absorption and ^{1}H and ^{13}C NMR spectroscopy techniques. We conclude that (αMe)Pro is able to explore both *trans*′ and *cis*′ ψ areas of the conformational space, but in (αMe)Pro the latter is overwhelmingly more populated, in marked contrast to the Pro preference. This finding is a clear indication that in (αMe)Pro the major 3D-structural determinant is the C^{α}-methyl group. The circular dichroism (CD) signature of a peptide type III′ β-turn conformation is also proposed.

Keywords: circular dichroism · conformation analysis · IR spectroscopy · NMR spectroscopy · X-ray diffraction

Introduction

In 1974, in their theoretical study on the effect of C^{α}-methylation on the energetically preferred conformations of L-Pro derivatives, Leach and co-workers predicted that this backbone substitution, producing C^{α}-methyl L-proline (L-(αMe)Pro), would generate a ϕ,ψ energy surface uniquely restricted to a single region, namely, that of the right-handed helical conformation.[1]

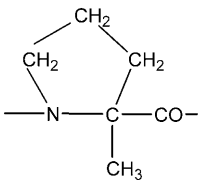

(αMe)Pro

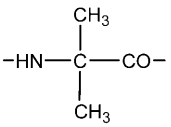

Aib

A decade later, Flippen-Anderson et al.,[2] by use of X-ray diffraction, showed that the simple, racemic "monopeptide" Ac-DL-(αMe)Pro-NHMe (Ac = acetyl; NHMe = methylamino) is indeed helical in the crystalline state (without any sta-

[a] M. D. Poli, Dr. A. Moretto, Dr. M. Crisma, Dr. C. Peggion, Prof. F. Formaggio, Prof. C. Toniolo
Institute of Biomolecular Chemistry, CNR
Padova Unit, Department of Chemistry
University of Padova
via Marzolo 1, 35131 Padova (Italy)
Fax: (+39) 049-827-5239
E-mail: claudio.toniolo@unipd.it

[b] Dr. B. Kaptein, Dr. Q. B. Broxterman
DSM Pharmaceutical Products
Innovative Synthesis and Catalysis
P.O. Box 18, 6160 MD Geleen (The Netherlands)

Supporting information for this article is available on the WWW under http://dx.doi.org/10.1002/chem.200900688.

bilization arising from a C=O···H–N intramolecular hydrogen bond) and its L-enantiomer adopts right-handedness. On the contrary, by use of conformational energy calculations, Delaney and Madison[3] demonstrated that the total energy for the L-enantiomer has a deep well at the right-handed C_7' (inverse γ turn) conformation.[4,5] For this compound both the semiextended (also termed poly(L-Pro)$_n$ II) and right-handed helical regions are less stable. However, the barrier separating the C_7' and helical regions is rather low and the population of the C_7' conformation tends to be overestimated in compounds too short to form β turns[6–8] or $3_{10}/\alpha$ helices.[9,10] From a combined ^{13}C NMR, IR absorption, and CD analysis these authors[3] confirmed the preference of Ac-L-(αMe)Pro-NHMe for the C_7' conformation, irrespective of the solvent used.

Only a few other studies, scattered and nonsystematic, have been subsequently reported on the conformational preferences of (αMe)Pro. This observation is surprising in that, among the C^α-methylated "monopeptides" of the coded amino acids, (αMe)Pro is by far the most conformationally restricted (the ϕ torsion angle is blocked; in linear peptides the preceding tertiary amide torsion angle ω can adopt only the *trans* conformation; the side-chain χ^n torsion angles are also rigidified).

Conformational potential-energy calculations suggested that poly-(L-(αMe)Pro)$_n$ is locked in the type II poly(L-Pro)$_n$ conformation.[11] The CD spectrum of a solution of poly-(L-(αMe)Pro)$_n$ of low molecular weight in alcohol, synthesized by means of N-carboxyanhydride polymerization, is reminiscent of that of type II poly(L-Pro)$_n$.[12] The preferred conformations of the heterochiral dipeptides Z-L-Pro-D-(αMe)Pro-NHMe (Z = benzyloxycarbonyl) and Z-D-(αMe)Pro-L-Pro-NHMe were examined by IR absorption and ^1H and ^{13}C NMR spectroscopic techniques.[13] The former adopts a type II β-turn conformation (in which D-(αMe)Pro is a left-handed helix), whereas in the latter the coexistence of at least four conformers was reported.

L-(αMe)Pro, inserted into a peptide antigen,[14,15] or at position 3 or 7 of the nonapeptide hormone bradykinin,[16–18] or in the NPNA-repeating motif of the *Plasmodium falciparium* protein,[19,20] was demonstrated by 2D NMR spectroscopy experiments to strongly stabilize β-turn conformations. Analogous results (β-turn formation and *trans*-L-Xxx-L-(αMe)Pro peptide bonds) were reported for L-(αMe)Pro-containing analogues of an antigen mimotope peptide[21] and the antimicrobial peptide buforin 2.[22] Interestingly, as opposed to the results from molecular-mechanics simulations, it was experimentally shown that the sequence L-(αMe)Pro-L-Pro is not tightly folded.[23] A combined molecular modeling and solution and crystal-state conformational study of acyl-L-Val-L-Xxx-NHR peptides (in which Xxx is 4-methylene-L-(αMe)Pro) suggests the absence of any C=O···H–N intramolecular hydrogen bond in this sequence.[24,25] According to the X-ray diffraction data, the 4-substituted L-(αMe)Pro residue is a right-handed helix.

Recently, the X-ray diffraction structure of *c*-(L-(αMe)Pro)$_2$ demonstrated the absence of epimerization in the course of 2,5-dioxopiperazine cyclization.[26] Using unnatural amino acid mutagenesis, L-(αMe)Pro and other modified Pro residues were incorporated in a member of the Cys-loop receptor protein superfamily.[27] L-Pro analogues, like L-(αMe)Pro, that strongly favor the *ω trans* conformer, were found to produce nonfunctional ion channels. Finally, in a DFT calculation study on Ac-L-(αMe)Pro-NHMe, in addition to not unexpected conclusions, such as that the replacement of the C^α hydrogen with a methyl in Pro destabilizes the *ω cis* conformation, a surprising structural finding associated with L-Pro C^α methylation was reported, namely, the stabilization of the poly(L-Pro)$_n$ II conformation, which was identified as an energy minimum for the L-(αMe)Pro "monopeptide," but not for those of the corresponding, unmethylated protein amino acid.[28]

Because of the published partially contradictory results mentioned above on the preferred conformation(s) of (αMe)Pro peptides, in this experimental work we decided to synthesize and investigate a large set of N^α-acylated, homo- and heterochiral dipeptide monoalkylamide systems of the type RCO-L (or D)-(αMe)Pro-Xxx-NHR′ and RCO-Xxx-L (or D)-(αMe)Pro-NHR′ (in which Xxx is L (or D)-Ala, Aib, or L (or D)-(αMe)Pro) long enough to fold into C=O···H–N intramolecularly hydrogen-bonded γ or β turns. The results are systematically compared with those obtained for the corresponding dipeptides based on the prototypical Pro, a well-known turn-forming residue.[29–39] We have chosen –NH*i*Pr (isopropylamino) as the C-terminal (and potential hydrogen-bonding donor) blocking group because it best mimics the continuation of the peptide main chain. The (αMe)Pro homo-dipeptides and the (αMe)Pro dipeptides containing the helicogenic Aib[40–43] combine two amino acids with a quaternary C^α atom. For the crystal-state 3D-structural analysis we used X-ray diffraction, whereas for our solution conformational study we relied heavily on FTIR absorption, NMR, and CD spectroscopic techniques. A limited part of this work has been reported in a preliminary form.[44,45]

Results and Discussion

Synthesis and characterization: D-(αMe)Pro and L-(αMe)Pro amide were obtained by amidase-catalyzed enzymatic resolution (Scheme 1).[46] Using the amidase from *Mycobacterium neoaurum* ATCC 25795, a conversion of 45% was obtained after 70 h (E ratio 240), whereas with the amidase from *Ochrobacterium anthropi* NCIMB 40321 (overexpressed in *E. coli*)[47] 48% conversion was reached after 26 h (E ratio 317). Note that whereas both amidases are in general L-selective for acyclic α-amino amides, for the (αMe)Pro amide the stereoselectivity is reversed. The H-DL-(αMe)Pro-NH_2 racemic substrate was obtained in 61% overall yield by base-catalyzed cyanoethylation of N-benzylidene-Ala amide, followed by acidic workup and ring-closing hydrogenation over palladium on charcoal.[48]

tert-Butyloxycarbonyl (*t*Boc) and benzyloxycarbonyl (Z) N-protected (αMe)Pro derivatives[49,50] were prepared with

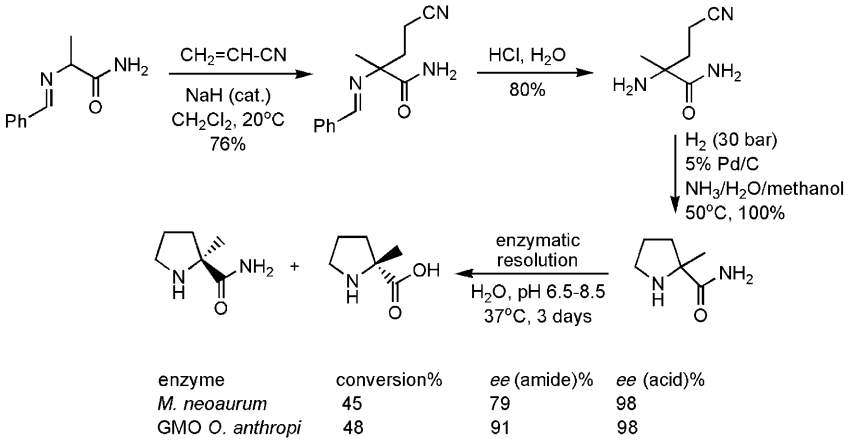

enzyme	conversion%	*ee* (amide)%	*ee* (acid)%
M. neoaurum	45	79	98
GMO *O. anthropi*	48	91	98

Scheme 1. Chemoenzymatic synthesis of D-(αMe)Pro and L-(αMe)Pro amide with the conversion and enantiomeric excess (*ee*) values.

use of *tert*-butyldicarbonate and N-(benzyloxycarbonyl) succinimide, respectively (Table S1 in the Supporting Information). The 3D structure of Z-D-(αMe)Pro-OH (crystals from methanol) was solved by X-ray diffraction (Figure 1). Interestingly, the tertiary Z-urethane function[51] is in the common *trans* conformation (Table S2 in the Supporting Information) in the crystal state, but two rotamers are present in a ratio of about (60–65)%:(40–35)% (ref. [13] and this work) in $CDCl_3$ and 55%:45% (this work) in CD_3OH, using the βCH_3 signal as the NMR spectroscopy probe. In the crystal the D-(αMe)Pro residue is a left-handed helix and the molecules are held together by means of intermolecular (carboxylic acid) OT···O0 (urethane) hydrogen bonds (Table S3 in the Supporting Information). The pyrrolidine ring is in a conformation intermediate between the $^3T_4$ (twist) and the E_4 (envelope).[52,53]

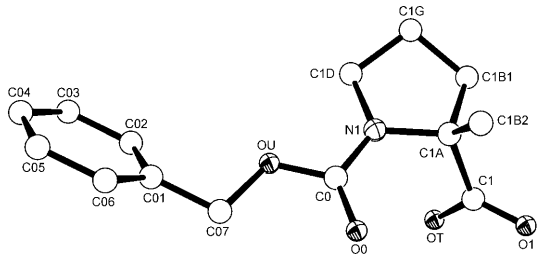

Figure 1. X-ray diffraction structure of Z-D-(αMe)Pro-OH with atom numbering.

In the (αMe)Pro-based compounds, peptide and isopropylamide bonds were formed by the 1-(3-dimethylamino)propyl-3-ethylcarbodiimide (EDC)/1-hydroxy-1,2,3-benzotriazole (HOBt)[54] or 7-aza-1-hydroxy-1,2,3-benzotriazole (HOAt)[55] C-activation method in CH_2Cl_2 in the presence of N-methylmorpholine. Despite the occurrence of the severely sterically demanding (αMe)Pro residue, coupling yields were from good to excellent (65–96%) with the single exception of that of the Aib-D-(αMe)Pro bond (24%). The *t*Boc and Z-urethane groups were removed by acidic treatment (HCl in diethyl ether) and by catalytic hydrogenation, respectively. N^{α}-Acetylation, isobutanoylation, and *para*-bromobenzoylation were performed on the N^{α}-deprotected (αMe)Pro isopropylamide or (αMe)Pro-containing dipeptide isopropylamides using the corresponding symmetrical anhydrides.

The physical properties and analytical data for the (αMe)Pro derivatives and peptides are listed in Table S1 in the Supporting Information. The syntheses and characterizations of *t*Boc-L-(αMe)Pro-OH,[49] Z-L-(αMe)Pro-OH,[50] and Z-D-(αMe)Pro-OH[12,13] have already been reported. All newly synthesized compounds were also characterized by ^1H NMR spectroscopy.

Crystal-state conformational analysis: We solved the X-ray diffraction structures of three novel, N^{α}-blocked, (αMe)Pro-containing dipeptide alkylamides, namely, *t*Boc-L-Ala-L-(αMe)Pro-NH*i*Pr, Z-Aib-D-(αMe)Pro-NH*i*Pr, and Z-D-(αMe)Pro-D-(αMe)Pro-NH*i*Pr. These crystal structures, combined with the five recently published by us,[40,41] Ac-L-Ala-L-(αMe)Pro-NH*i*Pr (Ac = acetyl), Ac-D-(αMe)Pro-D-Ala-NH*i*Pr, Ac-D-(αMe)Pro-L-Ala-NH*i*Pr, *i*Bu-L-Ala-D-(αMe)Pro-NH*i*Pr (*i*Bu = isobutanoyl), and Ac-D-(αMe)Pro-Aib-NH*i*Pr, offer an almost exhaustive overview of the conformations preferred by this sterically demanding amino acid. (The only missing, noncrystalline, dipeptide sequence in this list of X-ray diffraction structures is D-(αMe)Pro-L-(αMe)Pro or its L,D enantiomer.) In this work we have also solved the crystal structures of two N^{α}-blocked dipeptide alkylamides based on the related, coded amino acid Pro: Ac-Aib-L-Pro-NH*i*Pr and Z-L-Pro-D-Pro-NH*i*Pr. The molecular structures of the five new structures are illustrated in Figures 2, 3, 4, 5, and 6. The relevant N^{α}-blocking group and backbone torsion angles,[56] and the intra- and intermolecular hydrogen-bond parameters have been deposited (Tables S2 and S3, respectively, in the Supporting Information). Table 1 summarizes the ϕ,ψ torsion angles for all published (αMe)Pro-containing peptides and their related Pro analogues.

Figure 7 shows the average bond lengths and bond angles for the (αMe)Pro residue in comparison with those already reported[29] for Pro. All bond lengths and most of the bond angles closely match each other. Differences between 1.0 and 2.0° are found for the corresponding bond angles around the C^{α} atom (trisubstituted for Pro, but tetrasubstituted for (αMe)Pro). The steric effects of C^{α} tetrasubstitution may also account for the widening of the C^{α}-C′-O bond angle for (αMe)Pro as compared to Pro. The largest differ-

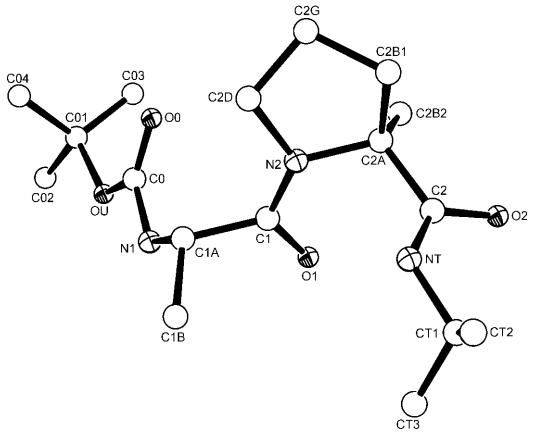

Figure 2. X-ray diffraction structure of *t*Boc-L-Ala-L-(αMe)Pro-NH*i*Pr with atom numbering.

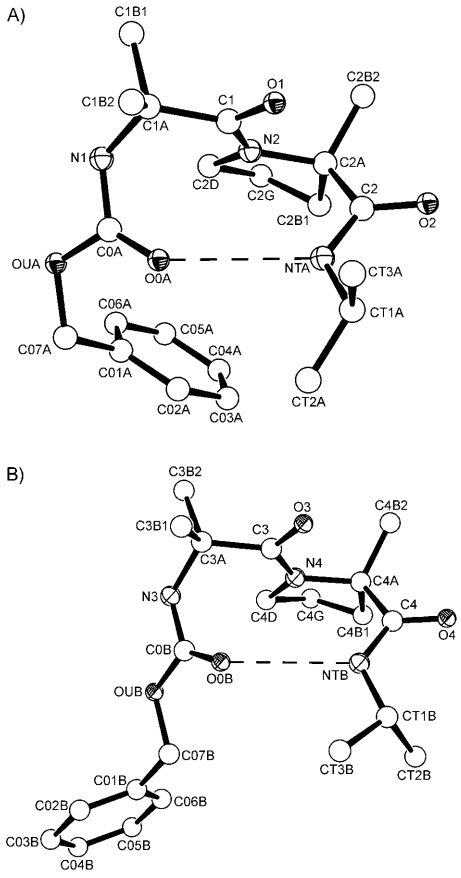

Figure 3. X-ray diffraction structures of the two independent molecules (A and B) in the asymmetric unit of Z-Aib-D-(αMe)Pro-NH*i*Pr with atom numbering. In each structure the C═O···H–N intramolecular hydrogen bond is represented by a dashed line.

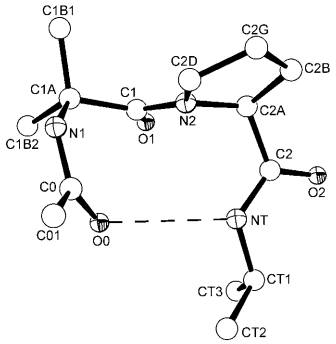

Figure 4. X-ray diffraction structure of Ac-Aib-L-Pro-NH*i*Pr with atom numbering. The second occupancy site of the Pro C$^{\gamma}$ atom is omitted for clarity. The C═O···H–N intramolecular hydrogen bond is represented by a dashed line.

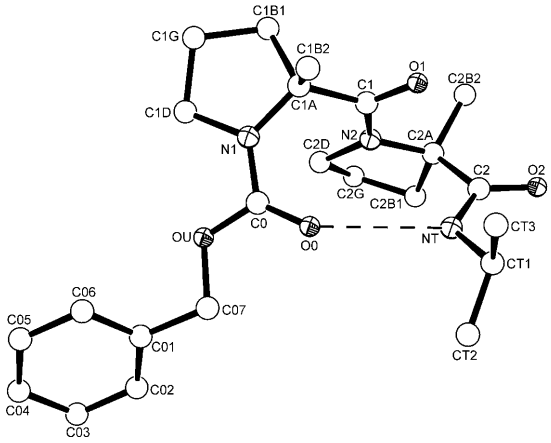

Figure 5. X-ray diffraction structure of Z-D-(αMe)Pro-D-(αMe)Pro-NH*i*Pr with atom numbering. The C═O···H–N intramolecular hydrogen bond is represented by a dashed line.

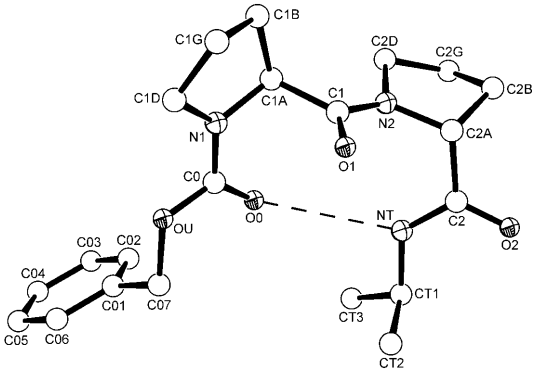

Figure 6. X-ray diffraction structure of Z-L-Pro-D-Pro-NH*i*Pr with atom numbering. The C═O···H–N intramolecular hydrogen bond is represented by a dashed line.

ence is observed for the endocyclic bond angle at C$^{\gamma}$, which is narrower by 3.3° for (αMe)Pro. However, this latter observation must be taken with caution, as it may be biased by static structural disorder of the Pro C$^{\gamma}$ atom (as often highlighted by anisotropic displacement parameters higher than those of the other ring atoms), which might result in an apparent ring flattening. Indeed, the sum of the average endocyclic bond angles is 525.2° for (αMe)Pro, but 529.4° for Pro. For comparison, in a planar, regular pentagon, the sum of the internal angles is 540°.

Table 1. 3D-structural parameters in the crystal state for the known Ala/(αMe)Pro, Ala/Pro, Aib/(αMe)Pro, Aib/Pro, (αMe)Pro–(αMe)Pro, and Pro–Pro N^{α}-blocked and C-amidated dipeptide sequences.

Dipeptide sequence	Backbone torsion angles				Type of turn	Reference
	ϕ_{i+1}	ψ_{i+1}	ϕ_{i+2}	ψ_{i+2}		
Ac-L-Ala-L-(αMe)Pro-NH*i*Pr	−135	77	−58	−37	–	[40]
*t*Boc-L-Ala-L-(αMe)Pro-NH*i*Pr	−76	130	−59	−36	–	this work
*i*Bu-L-Ala-L-Pro-NH*i*Pr	−129	76	−67	−22	–	[57]
Piv-D-Ala-D-Pro-NH*i*Pr[a]	74	−150	57	−142	–	[58]
	64	−152	83	−156	–	
Ac-D-(αMe)Pro-D-Ala-NH*i*Pr	53	32	66	25	β-III′	[40], [41]
Ac-L-Pro-L-Ala-NH*t*Bu[b]	−66	166	−71	154	–	[59]
*i*Bu-L-Pro-L-Ala-NH*i*Pr	−59	136	66	14	β-II	[60], [61]
Ac-D-(αMe)Pro-L-Ala-NH*i*Pr	53	−129	−77	−12	β-II′	[40], [41]
Z-D-Pro-L-Ala-NH*t*Bu	58	−137	−76	−14	β-II′	[59]
*i*Bu-L-Pro-D-Ala-NH*i*Pr	−62	137	96	3	β-II	[60], [61]
*i*Bu-L-Pro-D-Ala-NH*t*Bu	−60	133	82	15	β-II	[62]
*i*Bu-L-Ala-D-(αMe)Pro-NH*i*Pr	−55	133	78	0	β-II	[40], [41]
Piv-D-Ala-L-Pro-NH*i*Pr	60	−140	−89	9	β-II′	[63]
Ac-D-(αMe)Pro-Aib-NH*i*Pr	53	37	61	28	β-III′	[40], [41]
Piv-L-Pro-Aib-NHMe[c]	−58	139	61	25	β-II	[64]
Z-Aib-D-(αMe)Pro-NH*i*Pr	54	32	55	31	β-III′	this work
	51	39	67	22	β-III′	
Ac-Aib-L-Pro-NH*i*Pr	−50	−43	−80	−4	β-I	this work
Z-Aib-L-Pro-NHMe	−51	−40	−65	−25	β-III	[65]
Z-D-(αMe)Pro-D-(αMe)Pro-NH*i*Pr	50	34	57	28	β-III′	this work
Piv-L-Pro-L-Pro-NHMe	−60	138	−95	−7	–	[66]
Piv-L-Pro-D-Pro-NHMe	−58	134	83	−7	β-II	[66]
	−56	139	84	−14	β-II	
Z-L-Pro-D-Pro-NH*i*Pr	−58	141	82	−3	β-II	this work

[a] Piv = pivaloyl. [b] NH*t*Bu = *tert*-butylamino. [c] NHMe = methylamino.

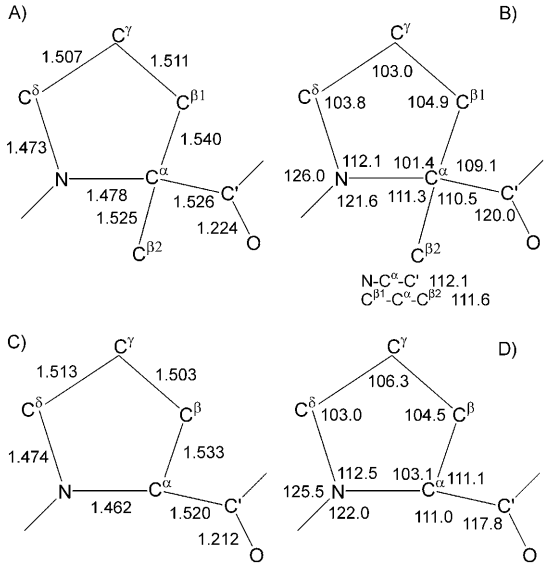

Figure 7. Average bond lengths in Å (A and C) and bond angles in degrees (B and D) for the (αMe)Pro and Pro[29,69] residues, respectively.

In the five (αMe)Pro-/Pro-containing structures reported in this paper, all (secondary and tertiary) urethane, amide, and peptide bonds (ω torsion angles) are in the usual *trans* conformation with modest deviations from the (180°) planarity ($|\Delta\omega| \leq 7.4°$), except for the amide ω_2 torsion angle of molecule **B** in the asymmetric unit of Z-Aib-D-(αMe)Pro-NH*i*Pr, 163.1(4)°. Four structures are folded in a β-turn conformation, which is stabilized by an $i \leftarrow i+3$ ((urethane or amide) C0=O0···H–NT (amide)) hydrogen bond of medium strength[67–69] (the O···N distances are in the range 2.997(5)–3.162(4) Å, and the O···H–N angles are between 148.6 and 162.3°). The only open structure is that of *t*Boc-L-Ala-L-(αMe)Pro-NH*i*Pr. The β turns formed by the homochiral -D-(αMe)Pro-D-(αMe)Pro- and the heterochiral -L-Pro-D-Pro- dipeptides are of type III′ and type II, respectively, as expected from their sequence chirality.[66] In both -Aib-D-(αMe)Pro- and -Aib-L-Pro- sequences, the achiral, helical Aib adopts the same screw sense as that of the following chiral residue, thus generating a type III′ β turn or a slightly distorted type I β turn, respectively. The difference, albeit small, between these two types of β turn points to a higher propensity for a regular helical conformation assignable to (αMe)Pro as compared to Pro. The only major conformational difference observed between molecules **A** and **B** of Z-Aib-D-(αMe)Pro-NH*i*Pr is found in the θ^2 torsion angle of the Z N^{α}-protecting group,[51] −69.5(6)° for molecule **A**, and −175.5(4)° for molecule **B**. All (αMe)Pro residues in these structures, including that of the open *t*Boc-L-Ala-L-(αMe)Pro-NH*i*Pr, are helical, with average ϕ,ψ torsion angles, |57.6°|, |30.2°|, remarkably close to those found experimentally for 3_{10}-helix peptides (57, 30°), but less near those of α-helix peptides (63, 42°).[9] It is worth pointing out that -D-(αMe)Pro-D-(αMe)Pro- is the first linear (αMe)Pro homopeptide sequence ever solved by X-ray diffraction. The Ala residue in *t*Boc-L-Ala-L-(αMe)Pro-NH*i*Pr and the N-terminal Pro residue in Z-L-Pro-D-Pro-NH*i*Pr adopt the semiextended conformation, whereas a conformation in the "bridge" region of the ϕ,ψ space[70] is seen for the C-terminal Pro residues of Ac-Aib-L-Pro-NH*i*Pr and Z-L-Pro-D-Pro-NH*i*Pr.

The pyrrolidine rings of the (αMe)Pro residues are $^{4}T_{3}$[52,53] in *t*Boc-L-Ala-L-(αMe)Pro-NH*i*Pr, and $^{3}T_{4}$ and $^{3}T_{4}/E_{4}$ in molecules **A** and **B**, respectively, of Z-Aib-D-(αMe)Pro-NH*i*Pr, whereas $^{3}T_{4}$ for both residues 1 and 2 of Z-D-(αMe)Pro-D-(αMe)Pro-NH*i*Pr. On the other hand, the pyrrolidine rings of the Pro residues are $E_{5}/^{1}T_{5}$ and $E_{1}/^{2}T_{1}$ for the two side-chain conformers of Ac-Aib-L-Pro-NH*i*Pr, and $^{3}T_{4}$ and $^{4}T_{3}$ for residues 1 and 2, respectively, of Z-L-Pro-D-Pro-NH*i*Pr.

Solution conformational analysis: We performed an extensive conformational analysis of the N^{α}-blocked dipeptide alkylamides based on (αMe)Pro and/or Pro residues in solution by use of FTIR absorption, NMR, and CD spectroscopic techniques.

The effects of replacing Pro with (αMe)Pro, sequence chirality, (αMe)Pro/Pro incorporation at position $i+1$ or $i+2$ in the sequence, and presence of the weakly turn former Ala or the much stronger turn former Aib[42–45] on the preferred conformation of model dipeptides are evident from the FTIR absorption spectra in $CDCl_3$ in the informative N–H stretching region, reported in Figures 8 and 9, as well as Figures S1 and S2 in the Supporting Information. We first

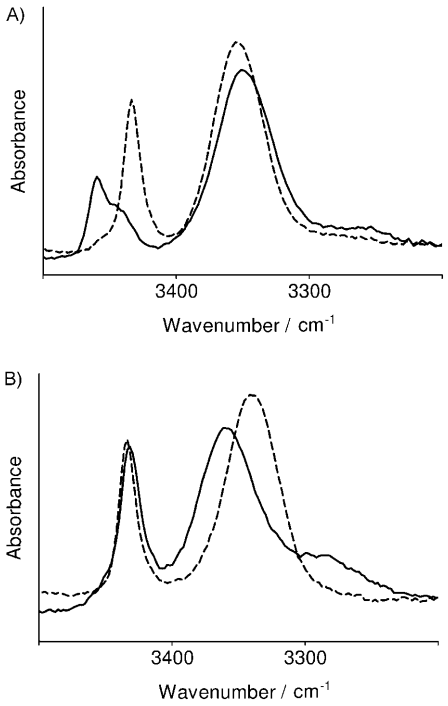

Figure 8. FTIR absorption spectra (3500–3200 cm^{-1} region) of A) Ac-D-(αMe)Pro-Aib-NH*i*Pr (solid line) and Ac-Aib-D-(αMe)Pro-NH*i*Pr (dashed line); and B) Ac-L-Pro-Aib-NH*i*Pr (solid line) and Ac-Aib-L-Pro-NH*i*Pr (dashed line) in $CDCl_3$ ([peptide] = 1 mM).

checked the concentration dependence (between 10 and 0.1 mM) in the spectra of all peptides investigated (not shown). The results indicate that at 1 mM concentration there is no evidence for significant self-association through intermolecular hydrogen bonding, that is, that all NH groups are either free (solvated by $CDCl_3$) or intramolecularly hydrogen bonded.

In general, the curves are characterized by two more or less intense bands, one located above 3400 cm^{-1} (free NHs) and the other below 3400 cm^{-1} (hydrogen-bonded NHs), respectively.[71–73] The following considerations can be drawn from our analysis: 1) As opposed to the homochiral sequences, the heterochiral sequences exhibit a higher tendency to fold. However, this conclusion does not apply to the two

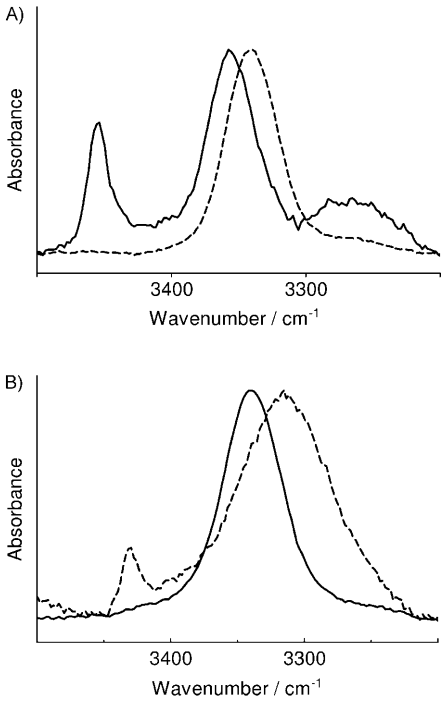

Figure 9. FTIR absorption spectra (3500–3200 cm^{-1} region) of: A) Ac-L-(αMe)Pro-D-(αMe)Pro-NH*i*Pr (solid line) and Ac-D-(αMe)Pro-D-(αMe)Pro-NH*i*Pr (dashed line); and B) Ac-L-Pro-D-Pro-NH*i*Pr (solid line) and Ac-D-Pro-D-Pro-NH*i*Pr (dashed line) in $CDCl_3$ ([peptide] = 1 mM).

-(αMe)Pro-(αMe)Pro- dipeptides, in which the opposite trend is found. 2) Turn formation is enhanced when (αMe)Pro replaces Pro in the sequence. 3) Positioning (αMe)Pro or Pro as residue $i+1$ is more favorable for folding than as residue $i+2$, particularly for (αMe)Pro. 4) The Aib/(αMe)Pro or Pro combination is more efficient in inducing a turn than the Ala/(αMe)Pro or Pro combination. 5) In the homo-dipeptides, the (αMe)Pro D,D and the Pro L,D stereoisomers appear to be folded to the highest extent observed in the present study (100%). This latter finding resembles that already reported for Z-L-Pro-D-(αMe)Pro-NHMe.[13]

Our conformational study of samples in $CDCl_3$ was extended to NMR spectroscopy. Not surprisingly, the NH chemical-shift perturbation trends observed in the titrations of the compounds studied in this work with the strong hydrogen-bond acceptor $^2H_6$ DMSO (dimethyl sulfoxide)[74,75] are often difficult to interpret, because in general the slopes are significantly reduced if the peptide main chain is short (as in our dipeptides)[73] and if the NH groups to be solvated by the perturbing agent are significantly shielded, for example, close to a sterically demanding α-amino acid, such as Aib and (αMe)Pro.

The NMR spectra of both Ac-D-Pro-D-Pro-NH*i*Pr and Ac-L-(αMe)Pro-D-(αMe)Pro-NH*i*Pr are complicated by *trans–cis* isomerism that generates multiple resonances. The differences in the chemical shifts observed for the isopropylamido NH proton of each conformer are $\Delta\delta = 0.9$ ppm ($\delta =$

7.74 and 6.84 ppm) and $\Delta\delta = 0.7$ ppm ($\delta = 6.55$ and 5.85 ppm), respectively. In addition, the ratios of the conformers are 1:0.86 and 1:0.21, respectively. Conversely, their diastereomers Ac-D-(αMe)Pro-D-(αMe)Pro-NH*i*Pr and Ac-L-Pro-D-Pro-NH*i*Pr exhibit much simpler NMR spectra, thus paralleling their FTIR absorption curves (Figure 9), indicative of a 100% population of C=O···H−N hydrogen-bonded folded conformers. For these diastereomers the chemical shifts of the isopropylamido NH proton single peak are seen at $\delta = 7.11$ and 7.06 ppm, respectively.

Complete assignments of the NMR signals were achieved by COSY, TOCSY, and HMBC experiments at 400 MHz. Figures 10 and 11, as well as Figure S3 in the Supporting Information, show the most conformationally informative sections of the ROESY spectra[76] of the homochiral (αMe)Pro homo-dipeptide, the heterochiral Pro homo-dipeptide, and the homo- and heterochiral -(αMe)Pro-Ala- dipeptides, respectively.

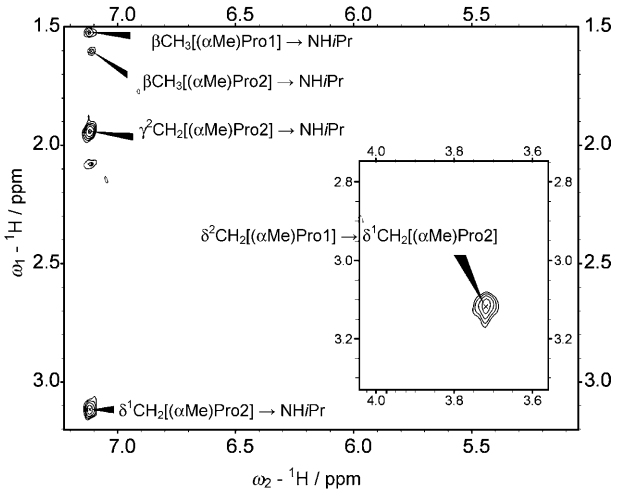

Figure 10. Sections of the ROESY spectrum of Ac-D-(αMe)Pro-D-(αMe)Pro-NH*i*Pr in $CDCl_3$ ([peptide] = 5 mM). The sequential connectivities βCH_3[(αMe)Pro2]→NH*i*Pr, γ^2CH_2[(αMe)Pro2]→NH*i*Pr, δ^1CH_2-[(αMe)Pro2]→NH*i*Pr, and δ^2CH_2[(αMe)Pro1]→δ^1CH_2[(αMe)Pro2] (inset) are indicated as well as the medium-range connectivity βCH_3-[(αMe)Pro1]→NH*i*Pr.

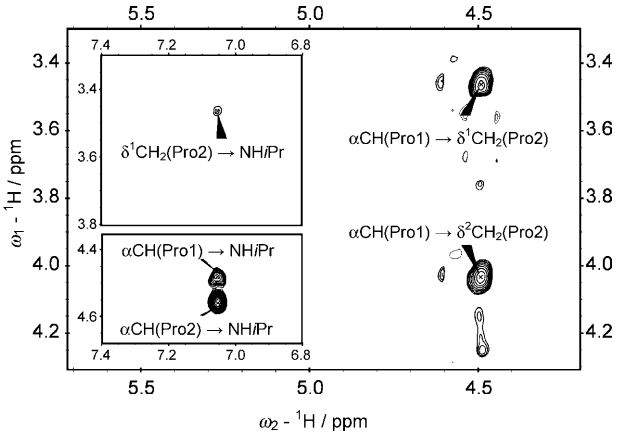

Figure 11. Sections of the ROESY spectrum of Ac-L-Pro-D-Pro-NH*i*Pr in $CDCl_3$ ([peptide] = 5 mM). The sequential connectivities αCH(Pro1)→$\delta^{1,2}CH_2$(Pro2), αCH(Pro2)→NH*i*Pr (inset, bottom), and δ^1CH_2(Pro2)→NH*i*Pr (inset, top) are indicated as well as the medium-range connectivity αCH(Pro1)→NH*i*Pr (inset, bottom).

A molecular model[13] and Figure 5 indicate that for the homochiral Ac-D-(αMe)Pro-D-(αMe)Pro-NH*i*Pr in a type III′ β-turn conformation, a strong sequential connectivity is expected between a δCH_2 proton of (αMe)Pro1 and a δCH_2 proton of (αMe)Pro2. This strong cross-peak is indeed observed (Figure 10), accompanied by additional, weaker (sequential and medium-range) cross-peaks involving the secondary amide NH proton. The chemical shift difference between the C^{β} and C^{γ} atoms ($\Delta\delta_{\beta\gamma}$) in Pro peptides has been shown to be correlated with the ψ torsion angle.[2,3,77–80] In this (αMe)Pro homo-dipeptide, we observed $\Delta\delta_{\beta\gamma}$ values of 12.3 and 14.1 ppm for (αMe)Pro1 and (αMe)Pro2, respectively. However, for (αMe)Pro-containing peptides this parameter is less conformationally indicative, as it is much larger than that of Pro-containing peptides ($8.0 < \Delta\delta_{\beta\gamma} < -7.0$), in particular due to a significant downfield variation in the chemical shift for the C^{β} atom associated with the presence of the βCH_3 substituent.[3]

A molecular model[81] and Figure 6 show that for the heterochiral Ac-L-Pro-D-Pro-NH*i*Pr in a type II β-turn conformation, two strong sequential connectivities are expected between the αCH(Pro1) and the $\delta^{1,2}CH_2$(Pro2) protons and between the αCH(Pro1) and NH(*i*Pr) protons. A weak sequential connectivity between a δCH_2(Pro2) proton and the NH(*i*Pr) proton should be also seen. In this conformation, the minimization of the pseudo A (1,3) strain between the L-Pro1 αCH proton and the D-Pro2 δ carbon restricts the rotation of the Pro1 torsion angle ψ to approximately 140° (semiextended conformation;[81] see also Table 1, and Table S3 in the Supporting Information). All of the above-mentioned cross-peaks are clearly apparent in Figure 11. In this dipeptide $\Delta\delta_{\beta\gamma}$ values of 3.1 and 5.5 ppm were seen for Pro1 and Pro2, respectively.[2,3,77–80] A molecular model (not shown) of Ac-L-(αMe)Pro-D-(αMe)Pro-NH*i*Pr indicates why this heterochiral dipeptide is not locked in the type II β-turn conformation, typical of the -L-Pro-D-Pro- sequence. The model shows a very short distance between the βCH_3 substituent of residue 1 and the δ carbon of residue 2.[13] Rotation of the (αMe)Pro1 ψ torsion angle out of the region of the semiextended conformation, required by the type II β turn for the $i+1$ position, can relieve this interaction. This finding is also consistent with the propensity of (αMe)Pro for the helical region of the conformational space.

All connectivities involving the ring protons of the (αMe)Pro2 residue seen in the ROESY spectrum of the type III′ β turn forming Ac-D-(αMe)Pro-D-(αMe)Pro-NH*i*Pr (Figure 10) are clearly missing in the corresponding spectrum of Ac-D-(αMe)Pro-D-Ala-NH*i*Pr (Figure S3, left, in the Supporting Information). However, both spectra do exhibit the only possible common connectivity, namely that between a βCH_3 proton of D-(αMe)Pro1 and the NH*i*Pr proton. Quite interestingly, if the structural restrictions imposed by the presence of the δCH_2 ring group of the (αMe)Pro2 resi-

due are removed, as in Ac-D-(αMe)Pro-L-Ala-NH*i*Pr, then D-(αMe)Pro1 can adopt the unusual semiextended conformation and the related -D-(αMe)Pro-L-Ala- sequence can fold in the type II′ β-turn conformation, typical of a -D,L-heterochiral sequence. Figure S3 (right, in the Supporting Information) shows that the cross-peak between a βCH_3 proton of D-(αMe)Pro1 and the NH*i*Pr proton is even more intense than the corresponding one in the homochiral sequence (Figure S3, left, in the Supporting Information). This observation is indeed expected on the basis of the related distances seen in the X-ray diffraction structures of these two -(αMe)Pro-Ala- dipeptides.[44,45] The $\Delta\delta_{\beta\gamma}$ values for the D-(αMe)Pro1 residue are 15.6 and 14.7 ppm for the homochiral -D-(αMe)Pro-D-Ala- and the heterochiral -D-(αMe)Pro-L-Ala- dipeptide sequences, respectively.

In summary, from our NMR spectroscopic data, it turns out that the 3D structures adopted by the (αMe)Pro-containing dipeptides in the crystalline state are highly (or exclusively) populated in $CDCl_3$ as well.

From our combined X-ray diffraction, FTIR absorption, and NMR spectroscopy work on Ac-D-(αMe)Pro-D-(αMe)Pro-NH*i*Pr discussed above, it turns out clearly that this simple dipeptide is unique in that its Z-protected analogue is rigidly folded in a single, left-handed type III′ β turn in the crystal state and it is fully folded in the same conformation in $CDCl_3$. Since the far-UV CD spectrum of a single type II β turn is well established,[82–84] but the spectra of type III and the closely related, nonhelical type I β turns have been the matter of controversy for a long time, in part due to the fact that not completely appropriate (long linear or cyclic) model peptides were utilized in those studies, we decided to take advantage of our short linear dipeptide to conclusively offer the correct CD spectrum for a type III/I β turn. To avoid any ambiguity, we used acetonitrile (MeCN), a solvent of low polarity (in this sense similar to $CDCl_3$), but (in contrast to $CDCl_3$) compatible with a CD measurement in the far-UV region. Figure 12 shows that the band of free NH groups is absent in the FTIR absorption spectrum in MeCN (only an intense band near 3330 cm^{-1} is seen), corroborating our data that this homochiral homo-dipeptide is 100% folded in an intramolecularly hydrogen-bonded β-turn conformation in a solvent of low polarity. The corresponding far-UV CD spectrum in MeCN (Figure 12) exhibits a very weak, positive shoulder at 225–230 nm followed by a remarkably strong positive Cotton effect centered at 216 nm and a weak Cotton effect of opposite sign at 202 nm. The crossover point between the two latter bands is seen at 205 nm. Obviously, in the CD spectrum of this D,D-configured dipeptide, the signs of all Cotton effects are opposite to those observed for the more common all-L peptides. Not surprisingly, the overall shape of the CD spectrum in Figure 12 closely resembles that of a 3_{10} helix.[85–87] Indeed, a type III/III′ β turn is the basic unit of the 3_{10} helix.[9] However, the positions of the Cotton effects and crossover point in the spectrum of our model dipeptide are significantly shifted (by about 8 nm) to longer wavelengths. This latter effect is not associated with the nature of the solvent, as the CD spectrum of this same dipeptide in MeOH (not shown) exhibits a very similar general shape.

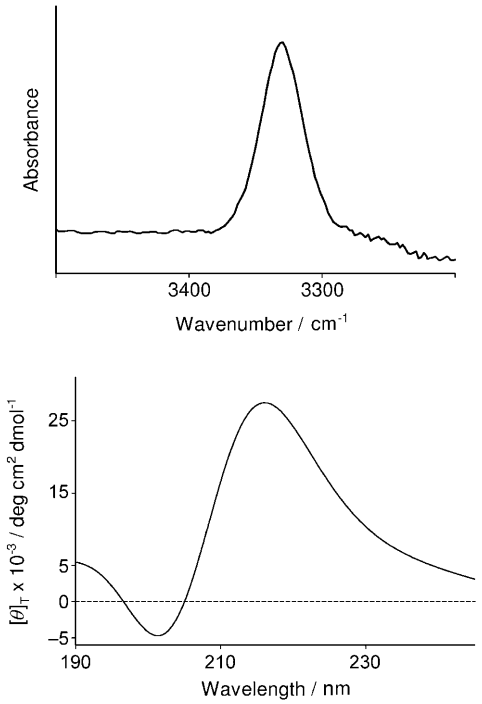

Figure 12. FTIR absorption spectrum (3500–3200 cm^{-1} region) (top) and far-UV CD spectrum (bottom) of Ac-D-(αMe)Pro-D-(αMe)Pro-NH*i*Pr in MeCN ([peptide] = 1 mM).

Conclusion

An analysis of our experimental data allows us to draw the following major conclusions:

1) Although the region of the (ϕ,ψ) conformational map overwhelmingly preferred by L-(αMe)Pro would indeed be that typical of right-handed $3_{10}/\alpha$ helices (with $\psi \approx -30°$ or *cis*′), as suggested in 1974 by Leach and co-workers,[1] the semiextended, type II poly(L-Pro)$_n$ region (with $\psi \approx 150°$ or *trans*′) can also be explored (although rarely) by this extremely sterically hindered C^α-tetrasubstituted α-amino acid. Conversely, the ϕ,ψ region ($\psi \approx 60°$), exactly halfway between the two regions discussed above and corresponding to the C_7' (inverse γ turn) conformation, does not seem to be accessible to L-(αMe)Pro.

2) In addition to the dramatic restriction of the ϕ torsion angle (to $\approx -60°$) by its five-membered pyrrolidine ring structure, L-(αMe)Pro undergoes rigidification of the preceding tertiary peptide bond (*trans*, or 180°, ω torsion angle) as well, as shown by all C^α-methylated L-α-amino acids investigated to date.

3) The known high propensity of the L-Pro residue for β-turn formation is even enhanced in peptides based on its C^α-methylated derivative when it is located at the $i+1$ corner position. Despite these characteristics, L-(αMe)Pro seems to be unable to nucleate a β turn when it is located at the $i+2$

corner position of a homochiral dipeptide sequence (with a coded amino acid at position $i+1$).

4) When incorporated at the $i+1$ corner position of the dipeptide sequence, L-(αMe)Pro tends to bias the β turn to its helical type (III), as opposed to the nonhelical type (II) typically induced by L-Pro.

To obtain conclusive information on the (αMe)Pro conformational preferences, we are currently actively working on the synthesis and 3D-structural characterization of the (αMe)Pro homo-oligopeptides longer than dimers. Our goal is to assess whether the semiextended (type II poly(L-Pro)$_n$) conformation would be populated at least under those "extreme" conditions of sequence, as anticipated in earlier theoretical[11] and experimental[12] papers, and re-proposed in recent conformational energy calculations.[28]

Experimental Section

Amino acid synthesis and resolution

N-Benzylidene-DL-(α-methyl)cyanoethylglycine amide: NaH (1.15 g, 0.04 mol, 60% in mineral oil) was added in small portions to a solution of N-benzylidene-DL-alanine amide (50 g, 0.28 mol) and acrylonitrile (19.6 mL, 0.31 mol) in CH_2Cl_2 (400 mL). The temperature was kept at 20°C with a cooling bath. After 3 h no more starting material was present according to TLC analyses. Then, the solution was washed with water (4×250 mL) and the aqueous layer was extracted with CH_2Cl_2 (3×250 mL). The solution was stirred overnight and the precipitated side-product (3-(benzylideamino)-3-methylglutaric imide) was filtered off. The solvent was removed under reduced pressure, affording an oil that was dissolved in methanol (120 mL). Addition of water (300 mL) then afforded a solid (49.4 g, 76%). ^{1}H NMR ($CDCl_3$, ^{2}H, 300 MHz), δ=8.26 (s, 1H; NH=C*H*), 7.81 (m, 2H; *ortho*-C_6H_5), 7.49 (m, 3H; *meta*- and *para*-C_6H_5), 7.35 (brs, 1H; CONH_2), 6.05 (brs, 1H; CONH_2), 2.44 (m, 3H; CH_2CH_2), 1.95 (m, 1H; CH_2CH_2), 1.54 ppm (s, 3H; CH_3).

DL-*(α-Methyl)cyanoethylglycine amide*: N-Benzylidene-DL-(α-methyl)cyanoethylglycine amide (48.55 g, 0.38 mol) was dissolved in CH_2Cl_2 (150 mL) and 4N HCl (70 mL, 1.2 equiv) was added under vigorous stirring. After stirring for 1 h, the organic and aqueous layers were separated. The organic layer was extracted with a 0.1N HCl solution and the two aqueous layers were combined. The acidic solution was made basic with 10N NaOH solution and concentrated under reduced pressure. The residue was dissolved in $CHCl_3$, and NaCl was filtered off. The organic layer was dried over Na_2SO_4 and evaporated to dryness. Yield: 23.7 g, 80%; ^{1}H NMR ($CDCl_3$, ^{2}H, 300 MHz), δ=7.30 and 5.83 (2brs, 2H; CONH_2); 2.44 (m, 2H; CH_2CH_2CN); 2.25 and 1.80 (m, 2H; CH_2CH$_2$CN); 1.49 (brs, 2H; CH_3CNH_2); 1.39 ppm (s, 3H; CH_3).

DL-*(α-Methyl)proline amide*: A 25% solution of NH_4OH (13 mL) and 5% Pd/C (4.7 g, Johnson Matthey type 39, 50% H_2O) were added to a solution of DL-(α-methyl)cyanoethylglycine amide (20 g, 0.14 mol) in MeOH (120 mL). The mixture was hydrogenated at 50°C and 30 bar of H_2 pressure in an autoclave. After 23 h the mixture was cooled down and the catalyst was filtered off through decalite. The solvent was removed under reduced pressure, affording the product as an oil. Yield: 18 g, 100%; ^{1}H NMR ($CDCl_3$, ^{2}H, 300 MHz), δ=7.70 and 5.25 (2brs, 2H; CONH_2); 3.10 and 2.85 (2m, 2H; CCH$_2$CH$_2$CH_2); 2.25–1.60 (m, 5H; CCH_2CH_2CH$_2$NH); 1.41 ppm (s, 3H; CH_3).

Enzymatic resolution of DL-(α-methyl)proline amide using *Mycobacterium neoaurum*: The above amide (15 g, 0.117 mol) was dissolved in H_2O and the pH was adjusted to 8.5 by addition of acetic acid. Freeze-dried whole cells of *M. neoaurum* (1.5 g) were added and the mixture was shaken at 37°C. The reaction was stopped after 70 h when the conversion was 48%, according to the ammonia determination method. The cell mass was removed by centrifugation, and ion-exchange chromatography with the strongly basic resin Amberlyst A-26 was used to separate the carboxylic acid and its amide. The amide was recovered by eluting with water, and the carboxylic acid after eluting with 1N acetic acid. The two fractions were evaporated to dryness, affording 7.3 g (49%) of L-amide (79% *ee*) and 7.7 g (51%) of D-carboxylic acid (98% *ee*). The conversion based on the enantiomeric excess (*ee*) was 45%. The carboxylic acid was then stirred in cold *i*PrOH (50 mL) for 3 h, and filtered off as a solid (4.6 g, 30%). ^{1}H NMR (D_2O, 300 MHz): δ=3.31 (m, 2H; CCH$_2$CH$_2$CH_2), 2.27–1.88 (m, 4H; CCH_2CH_2CH$_2$), 1.52 ppm (s, 3H; CH_3).

Enzymatic resolution of DL-(α-methyl)proline amide using *Ochrobactrum anthropi*: The amide (1.00 g, 7.8 mmol) was dissolved in an aqueous solution of $ZnSO_4$ (1 mM, 10 g) and the pH was adjusted to 6.5 by addition of acetic acid. The amidase of *O. anthropi*, overexpressed in *E. coli* (20 μL cell-free extract), was added and the mixture was shaken at 37°C. After 26 h a conversion of 45% was reached, according to the ammonia determination method. The reaction products were analyzed by HPLC: D-carboxylic acid 98% *ee* and L-amide 91% *ee* The conversion based on the *ee* was 48%. For the workup, see above.

HPLC method for the enantiomeric excess determination: Column: Astec CLC-L (150×4.6 mm i.d.); column temperature: 45°C; eluant: 2 mM $CuSO_4$ in Mili-Q water; flow: 1.5 mL min^{-1}; detection UV: λ=254 nm.

X-ray diffraction: Colorless crystals of Z-D-(αMe)Pro-OH, *t*Boc-L-Ala-L-(αMe)Pro-NH*i*Pr, Z-Aib-D-(αMe)Pro-NH*i*Pr, Ac-Aib-L-Pro-NH*i*Pr, Z-D-(αMe)Pro-D-(αMe)Pro-NH*i*Pr, and Z-L-Pro-D-Pro-NH*i*Pr were grown by slow evaporation from MeOH, acetone, ethyl acetate, wet MeOH, chloroform, and ethyl acetate, respectively. Diffraction data were collected at room temperature using a Philips PW1100 diffractometer in the θ–2θ scan mode up to 2θ=120°, using graphite-monochromated $Cu_{K\alpha}$ radiation (λ=1.54178 Å). Intensities were corrected for Lorentz and polarization effects, not for absorption. All structures were solved by direct methods by use of the SIR 2002[88] program. Refinements were carried out on F^2 by full-matrix block least-squares, with use of all data, by application of the SHELXL 97[89] program with all non-hydrogen atoms anisotropic, and their positional parameters and the anisotropic displacement parameters being allowed to refine at alternate cycles. Hydrogen atoms of all peptide molecules were calculated at idealized positions and refined using a riding model. The hydrogen atoms of the water molecule cocrystallized with *t*Boc-L-Ala-L-(αMe)Pro-NH*i*Pr were located on a ΔF map and their positional parameters were not refined. The hydrogen atoms of the water molecule cocrystallized with Ac-Aib-L-Pro-NH*i*Pr were located on a ΔF map and isotropically refined. The Pro C$^{\gamma}$ atom of the same peptide was refined on two sites (atoms C2G and C2G′), each with 0.5 occupancy.

Z-D-(αMe)Pro-OH: $C_{14}H_{17}NO_4$; crystal size 0.50×0.45×0.35 mm; orthorhombic; space group $P2_12_12_1$; a=7.287(2), b=8.256(2), c=22.860(4) Å; V=1375.3(6) Å^3; Z=4; ρ_{calcd}=1.272 Mg m^{-3}; μ=0.773 mm^{-1}; 1411 collected reflections; 1377 independent reflections (R_{int}=0.048); data/parameters 1377/161; R_1=0.047 with $I\geq 2\sigma(I)$; wR_2=0.139 (on F^2, all data); goodness-of-fit on F^2 1.186; residual electron density 0.216/−177 e Å^{-3}.

t*Boc-L-Ala-L-(αMe)Pro-NHiPr monohydrate*: $C_{17}H_{33}N_3O_5$; crystal size 0.40×0.30×0.20 mm; monoclinic; space group $P2_1$; a=6.514(2), b=13.794(3), c=11.847(3) Å; β=95.84(4)°; V=1059.0(5) Å^3; Z=2; ρ_{calcd}=1.127 Mg m^{-3}; μ=0.678 mm^{-1}; 1864 collected reflections; 1788 independent reflections (R_{int}=0.087); data/parameters 1788/227; R_1=0.066 with $I\geq 2\sigma(I)$; wR_2=0.181 (on F^2, all data); goodness-of-fit on F^2 1.107; residual electron density 0.267/−348 e Å^{-3}.

Z-Aib-D-(αMe)Pro-NHiPr: $C_{21}H_{31}N_3O_4$; crystal size 0.50×0.40×0.25 mm; orthorhombic; space group $P2_12_12_1$; a=9.172(2), b=10.921(2), c=42.936(5) Å; V=4300.8(13) Å^3; Z=8; ρ_{calcd}=1.203 Mg m^{-3}; μ=0.678 mm^{-1}; 4172 collected reflections; 4070 independent reflections (R_{int}=0.036); data/parameters 4070/482; R_1=0.054 with $I\geq 2\sigma(I)$; wR_2=0.159 (on F^2, all data); goodness-of-fit on F^2 1.079; residual electron density 0.189/−193 e Å^{-3}.

Ac-Aib-L-Pro-NHiPr monohydrate: $C_{14}H_{27}N_3O_4$; crystal size 0.50×0.25×0.20 mm; monoclinic; space group $P2_1$; a=8.336(1), b=12.996(3), c=8.816(2) Å, β=116.91(4)°; V=851.7(3) Å^3; Z=2; ρ_{calcd}=1.175 Mg m^{-3}; μ=0.707 mm^{-1}; 1523 collected reflections; 1439 independent reflections

($R_{int}=0.134$); data/parameters 1439/211; $R_1=0.059$ with $I\geq 2\sigma(I)$; $wR_2=0.165$ (on F^2, all data); goodness-of-fit on F^2 1.056; residual electron density 0.264/−301 e Å^{-3}.

Z-D-(*αMe*)*Pro*-D-(*αMe*)*Pro*-*NHiPr*: $C_{23}H_{33}N_3O_4$; crystal size $0.45\times0.35\times0.20$ mm; monoclinic; space group $P2_1$; $a=9.473(2)$, $b=10.594(3)$, $c=12.082(3)$ Å, $\beta=108.40(8)°$; $V=1150.5(5)$ Å^3; $Z=2$; $\rho_{calcd}=1.199$ Mg m^{-3}; $\mu=0.665$ mm^{-1}; 2068 collected reflections; 1986 independent reflections ($R_{int}=0.063$); data/parameters 1986/260; $R_1=0.083$ with $I\geq 2\sigma(I)$; $wR_2=0.221$ (on F^2, all data); goodness-of-fit on F^2 1.084; residual electron density 0.304/−290 e Å^{-3}.

Z-L-*Pro*-D-*Pro*-*NHiPr*: $C_{21}H_{29}N_3O_4$; crystal size $0.40\times0.40\times0.25$ mm; monoclinic; space group $P2_1$; $a=10.321(3)$, $b=9.746(3)$, $c=11.465(3)$ Å; $\beta=115.34(7)°$; $V=1042.3(5)$ Å^3; $Z=2$; $\rho_{calcd}=1.235$ Mg m^{-3}; $\mu=0.699$ mm^{-1}; 1925 collected reflections; 1839 independent reflections ($R_{int}=0.064$); data/parameters 1839/254; $R_1=0.046$ with $I\geq 2\sigma(I)$; $wR_2=0.127$ (on F^2, all data); goodness-of-fit on F^2 1.055; residual electron density 0.168/−185 e Å^{-3}.

CCDC 711587, 711588, 711589, 711590, 711591, and 711592 contain the supplementary crystallographic data for this paper. These data can be obtained from The Cambridge Crystallographic Data Centre by visiting www.ccdc.cam.ac.uk/data_request/cif.

FTIR absorption spectroscopy: FTIR absorption spectra were recorded using a Perkin–Elmer 1720 X FTIR spectrophotometer, nitrogen-flushed, with a sample shuttle device and at 2 cm^{-1} nominal resolution, averaging 100 scans. Solvent (baseline) spectra were recorded under the same conditions. Cells with CaF_2 windows and path lengths of 0.1, 1.0, and 10 mm were used. Spectrograde deuterochloroform (99.8%, ^{2}H) was obtained from Fluka.

NMR spectroscopy: ^{1}H NMR spectra were recorded using a Bruker AM 400 spectrometer. Measurements were carried out in $CDCl_3$ (99.96% ^{2}H from Acros Organics) and DMSO (99.96% $^2H_6$ from Acros Organics).

Circular dichroism spectroscopy: The CD spectra were obtained using a Jasco J-715 dichrograph. Cylindrical, fused quartz cells of 1.0, 0.2, and 0.1 mm path lengths (Hellma) were used. The values are expressed in terms of $[\Theta]_T$, the total molar ellipticity (deg cm^2 dmol^{-1}). Spectrograde acetonitrile (Acros Organics) was used as solvent.

Acknowledgements

The authors are grateful to the Padova trainees Andrea Dalla Bona and Erika Andreetto who developed the synthesis of (αMe)Pro during their internships at DSM.

[1] A. Burgess, Y. Paterson, S. J. Leach in *Peptides, Polypeptides, and Proteins* (Eds.: E. R. Blout, F. A. Bovey, M. Goodman, N. Lotan), Wiley, New York, **1974**, pp. 79–87.
[2] J. L. Flippen-Anderson, R. Gilardi, I. L. Karle, M. H. Frey, S. J. Opella, L. M. Gierasch, M. Goodman, V. Madison, N. G. Delaney, *J. Am. Chem. Soc.* **1983**, *105*, 6609–6614.
[3] N. G. Delaney, V. Madison, *J. Am. Chem. Soc.* **1982**, *104*, 6635–6641.
[4] G. Némethy, M. P. Printz, *Macromolecules* **1972**, *5*, 755–758.
[5] B. W. Matthews, *Macromolecules* **1972**, *5*, 818–819.
[6] C. M. Venkatachalam, *Biopolymers* **1968**, *6*, 1425–1436.
[7] C. Toniolo, *Crit. Rev. Biochem.* **1980**, *9*, 1–44.
[8] G. D. Rose, L. M. Gierasch, J. A. Smith, *Adv. Protein Chem.* **1985**, *38*, 1–109.
[9] C. Toniolo, E. Benedetti, *Trends Biochem. Sci.* **1991**, *16*, 350–353.
[10] K. A. Bolin, G. Millhauser, *Acc. Chem. Res.* **1999**, *32*, 1027–1033.
[11] C. M. Venkatachalam, cited in ref. [12].
[12] C. G. Overberger, Y. S. Jon, *J. Polym. Sci. Polym. Chem. Edit.* **1977**, *15*, 1413–1421.
[13] P. W. Baures, W. H. Ojala, W. B. Gleason, R. L. Johnson, *J. Pept. Res.* **1997**, *49*, 1–13.
[14] N. G. J. Richards, M. G. Hinds, D. M. Brennand, M. J. Glennie, J. H. Welsh, J. A. Robinson, *Biochem. Pharmacol.* **1990**, *40*, 119–123.
[15] M. G. Hinds, J. H. Welsh, D. M. Brennand, J. Fisher, M. J. Glennie, N. G. J. Richards, D. L. Turner, J. A. Robinson, *J. Med. Chem.* **1991**, *34*, 1777–1789.
[16] J. H. Welsh, O. Zerbe, W. von Philipsborn, J. A. Robinson, *FEBS Lett.* **1992**, *297*, 216–220.
[17] O. Zerbe, J. H. Welsh, J. A. Robinson, W. von Philipsborn, *Magn. Reson. Chem.* **1992**, *30*, 683–685.
[18] O. Zerbe, J. H. Welsh, J. A. Robinson, W. von Philipsborn, *J. Magn. Reson.* **1992**, *100*, 329–335.
[19] C. Bisang, C. Weber, J. Inglis, C. A. Schiffer, W. F. van Gunsteren, I. Jelesarov, H. R. Bosshard, J. A. Robinson, *J. Am. Chem. Soc.* **1995**, *117*, 7904–7915.
[20] A. P. Nanzer, A. E. Torda, C. Bisang, C. Weber, J. A. Robinson, W. F. van Gunsteren, *J. Mol. Biol.* **1997**, *267*, 1012–1025.
[21] D. S. Sem, B. L. Baker, E. J. Victoria, D. S. Jones, D. Marquis, L. Yu, J. Parks, S. M. Coutts, *Biochemistry* **1998**, *37*, 16069–16081.
[22] S. Kobayashi, A. Chikushi, S. Tougu, Y. Imura, M. Nishida, Y. Yano, K. Matsuzaki, *Biochemistry* **2004**, *43*, 15610–15616.
[23] D. Gani, A. Lewis, T. Rutherford, J. Wilkie, I. Stirling, T. Jenn, M. D. Ryan, *Tetrahedron* **1998**, *54*, 15793–15819.
[24] D. Balducci, E. Emer, F. Piccinelli, G. Porzi, M. Recanatini, S. Sandri, *Tetrahedron: Asymmetry* **2005**, *16*, 3785–3794.
[25] D. Balducci, A. Bottoni, M. Calvaresi, G. Porzi, S. Sandri, *Tetrahedron: Asymmetry* **2006**, *17*, 3273–3281.
[26] M. Jainta, M. Nieger, S. Bräse, *Eur. J. Org. Chem.* **2008**, 5418–5424.
[27] S. C. R. Lummis, D. L. Beene, L. W. Lee, H. A. Lester, R. W. Broadhurst, D. A. Dougherty, *Nature* **2005**, *438*, 248–250.
[28] A. Flores-Ortega, A. I. Jiménez, C. Cativiela, R. Nussinov, C. Alemán, J. Casanovas, *J. Org. Chem.* **2008**, *73*, 3418–3427.
[29] E. Benedetti, A. Bavoso, B. Di Blasio, V. Pavone, C. Pedone, C. Toniolo, G. M. Bonora, *Biopolymers* **1983**, *22*, 305–317.
[30] I. L. Karle, J. Flippen-Anderson, M. Sukumar, P. Balaram, *Proc. Natl. Acad. Sci. USA* **1987**, *84*, 5087–5091.
[31] B. Di Blasio, V. Pavone, M. Saviano, A. Lombardi, F. Nastri, C. Pedone, E. Benedetti, M. Crisma, M. Anzolin, C. Toniolo, *J. Am. Chem. Soc.* **1992**, *114*, 6273–6278.
[32] K. A. Williams, C. M. Deber, *Biochemistry* **1991**, *30*, 8919–8923.
[33] M. W. MacArthur, J. M. Thornton, *J. Mol. Biol.* **1991**, *218*, 397–412.
[34] A. Yaron, F. Naider, *Crit. Rev. Biochem. Mol. Biol.* **1993**, *28*, 31–81.
[35] A. A. Adzhubei, M. J. E. Sternberg, *J. Mol. Biol.* **1993**, *229*, 472–493.
[36] M. P. Williamson, *Biochem. J.* **1994**, *297*, 249–260.
[37] D. Pal, P. Chakrabarti, *J. Mol. Biol.* **1999**, *294*, 271–288.
[38] S. J. Eyles, L. M. Gierasch, *J. Mol. Biol.* **2000**, *301*, 737–747.
[39] R. Berisio, S. Loguercio, A. De Simone, A. Zagari, L. Vitagliano, *Protein Pept. Lett.* **2006**, *13*, 847–854.
[40] C. Toniolo, *Biopolymers* **1989**, *28*, 247–257.
[41] I. L. Karle, P. Balaram, *Biochemistry* **1990**, *29*, 6747–6756.
[42] C. Toniolo, M. Crisma, F. Formaggio, C. Peggion, *Biopolymers* **2001**, *60*, 396–419.
[43] C. Toniolo, M. Crisma, G. M. Bonora, E. Benedetti, B. Di Blasio, V. Pavone, C. Pedone, A. Santini, *Biopolymers* **1991**, *31*, 129–138.
[44] C. Toniolo, A. Moretto, M. Crisma, F. Formaggio, B. Kaptein, Q. B. Broxterman in Proc. 4th Int. Pept. Symp. 2007 (Ed.: J. Wilce), Australian Peptide Association, Melbourne, Australia, **2008**, K360, http://www.peptideoz.org (online only).
[45] A. Moretto, F. Terrenzani, M. Crisma, F. Formaggio, B. Kaptein, Q. B. Broxterman, C. Toniolo, *Biopolymers* **2008**, *89*, 465–470.
[46] T. Sonke, B. Kaptein, W. H. J. Boesten, Q. B. Broxterman, J. Kamphuis, F. Formaggio, C. Toniolo, F. P. J. T. Rutjes, H. E. Schoemaker in *Stereoselective Catalysis* (Ed.: N. K. Patel), Dekker, New York, **2000**, pp. 23–58.
[47] T. Sonke, S. Ernste, R. F. Tandler, B. Kaptein, W. P. H. Peeters, F. B. J. Van Assema, M. G. Wubbolts, H. Schoemaker, *Appl. Environ. Microbiol.* **2005**, *71*, 7961–7973.

[48] B. Kaptein, Q. B. Broxterman, H. E. Schoemaker, F. P. J. T. Rutjes, J. J. N. Veerman, J. Kamphuis, C. Peggion, F. Formaggio, C. Toniolo, *Tetrahedron* **2001**, *57*, 6567–6577.
[49] S. Thaisrivongs, D. T. Pals, J. A. Lawson, S. R. Turner, D. W. Harris, *J. Med. Chem.* **1987**, *30*, 536–541.
[50] S. T. Tong, P. W. R. Harris, D. Barker, M. A. Brimble, *Eur. J. Org. Chem.* **2008**, 164–170.
[51] E. Benedetti, C. Pedone, C. Toniolo, M. Dudek, G. Némethy, M. S. Pottle, H. A. Scheraga, *Int. J. Pept. Protein Res.* **1983**, *21*, 163–181.
[52] T. Ashida, M. Kakudo, *Bull. Chem. Soc. Jpn.* **1974**, *47*, 1129–1133.
[53] D. Cremer, J. A. Pople, *J. Am. Chem. Soc.* **1975**, *97*, 1354–1358.
[54] W. König, R. Geiger, *Chem. Ber.* **1970**, *103*, 788–798.
[55] L. A. Carpino, *J. Am. Chem. Soc.* **1993**, *115*, 4397–4398.
[56] IUPAC-IUB Commission on Biochemical Nomenclature: *Biochemistry* **1970**, *9*, 3471–3479.
[57] A. Aubry, J. Protas, M. Boussard, M. Marraud, *Acta Crystallogr. Sect. A* **1980**, *36*, 2825–2827.
[58] A. Aubry, J. Protas, M. Boussard, M. Marraud, *Acta Crystallogr. Sect. A* **1980**, *36*, 321–326.
[59] M. Crisma, G. Valle, A. Bianco, F. Formaggio, C. Toniolo, *Z. Kristallogr.* **1997**, *212*, 465–471.
[60] A. Aubry, J. Protas, M. Boussard, M. Marraud, *Acta Crystallogr. Sect. A* **1977**, *33*, 2399–2406.
[61] A. Aubry, M. T. Cung, M. Marraud, *J. Am. Chem. Soc.* **1985**, *107*, 7640–7647.
[62] A. Bianco, T. Bertolini, M. Crisma, G. Valle, C. Toniolo, M. Maggini, G. Scorrano, M. Prato, *J. Pept. Res.* **1997**, *49*, 159–170.
[63] A. Aubry, J. Protas, M. Boussard, M. Marraud, *Acta Crystallogr. Sect. A* **1979**, *35*, 694–699.
[64] B. V. Venkataram Prasad, H. Balaram, P. Balaram, *Biopolymers* **1982**, *21*, 1261–1273.
[65] B. V. Venkataram Prasad, N. Shamala, R. Nagaraj, R. Chandrasekaran, P. Balaram, *Biopolymers* **1979**, *18*, 1635–1646.
[66] A. Aubry, B. Vitoux, M. Marraud, *Biopolymers* **1985**, *24*, 1089–1100.
[67] C. Ramakrishnan, N. Prasad, *Int. J. Protein Res.* **1971**, *3*, 209–231.
[68] R. Taylor, O. Kennard, W. Versichel, *Acta Crystallogr. Sect. A* **1984**, *40*, 280–288.
[69] C. H. Görbitz, *Acta Crystallogr. Sect. A* **1989**, *45*, 390–395.
[70] S. S. Zimmerman, M. S. Pottle, G. Némethy, H. A. Scheraga, *Macromolecules* **1977**, *10*, 1–9.
[71] M. T. Cung, M. Marraud, J. Néel, *Ann. Chim.* **1972**, 183–209.
[72] E. S. Pysh, C. Toniolo, *J. Am. Chem. Soc.* **1977**, *99*, 6211–6219.
[73] C. Toniolo, G. M. Bonora, V. Barone, A. Bavoso, E. Benedetti, B. Di Blasio, P. Grimaldi, F. Lelj, V. Pavone, C. Pedone, *Macromolecules* **1985**, *18*, 895–902.
[74] K. D. Kopple, M. Ohnishi, A. Go, *Biochemistry* **1969**, *8*, 4087–4095.
[75] D. Martin, H. G. Hauthal, *Dimethyl Sulphoxide*, Van Nostrand Reinhold, Wokingham, **1975**.
[76] K. Wüthrich in *NMR of Proteins and Nucleic Acids*, Wiley, New York, **1986**, pp. 192–196.
[77] I. Z. Siemion, Th. Wieland, K. H. Pook, *Angew. Chem.* **1975**, *87*, 712–714; *Angew. Chem. Int. Ed. Engl.* **1975**, *14*, 702–703.
[78] C. M. Deber, V. Madison, E. R. Blout, *Acc. Chem. Res.* **1976**, *9*, 106–113.
[79] V. Madison, K. D. Kopple, *J. Am. Chem. Soc.* **1980**, *102*, 4855–4863.
[80] L. M. Gierasch, C. M. Deber, V. Madison, C.-H. Niu, E. R. Blout, *Biochemistry* **1981**, *20*, 4730–4738.
[81] J. S. Madalengoitia, *J. Am. Chem. Soc.* **2000**, *122*, 4986–4987.
[82] R. Woody in *Peptides, Polypeptides, and Proteins* (Eds.: E. R. Blout, F. A. Bovey, N. Lotan, M. Goodman), Wiley, New York, **1974**, pp. 338–350.
[83] A. Perczel, M. Hollosi in *Circular Dichroism and the Conformational Analysis of Biomolecules* (Ed.: G. D. Fasman), Plenum Press, New York, **1996**, pp. 285–380.
[84] E. Vass, M. Hollosi, F. Besson, R. Buchet, *Chem. Rev.* **2003**, *103*, 1917–1954.
[85] M. Manning, R. W. Woody, *Biopolymers* **1991**, *31*, 569–586.
[86] C. Toniolo, A. Polese, F. Formaggio, M. Crisma, J. Kamphuis, *J. Am. Chem. Soc.* **1996**, *118*, 2744–2745.
[87] F. Formaggio, M. Crisma, P. Rossi, P. Scrimin, B. Kaptein, Q. B. Broxterman, J. Kamphuis, C. Toniolo, *Chem. Eur. J.* **2000**, *6*, 4498–4504.
[88] M. C. Burla, M. Camalli, B. Carrozzini, G. L. Cascarano, C. Giacovazzo, G. Polidori, R. Spagna, *J. Appl. Crystallogr.* **2003**, *36*, 1103.
[89] G. M. Sheldrick, *Acta Crystallogr. Sect. A* **2008**, *64*, 112–122.

Received: March 17, 2009
Published online: July 3, 2009

